An 85–116 GHz SIS Receiver Using Inductively Shunted Edge Junctions

SHING-KUO PAN, MEMBER, IEEE, ANTHONY R. KERR, FELLOW, IEEE, MARC J. FELDMAN, MEMBER, IEEE, ALAN W. KLEINSASSER, JAMES W. STASIAK, ROBERT L. SANDSTROM, ASSOCIATE MEMBER, IEEE, AND WILLIAM J. GALLAGHER, MEMBER, IEEE

Abstract—**For the most part, SIS receivers have failed by a wide margin to achieve the sensitivity promised by theory. One of the main reasons for this is the difficulty of providing appropriate embedding impedances at the signal and image frequencies and at the higher harmonic sidebands. We describe an SIS mixer with a broad-band integrated tuning structure. The mixer is tunable from 85 to 116 GHz and at 114 GHz has a noise temperature ≤ 5.6 K DSB and unity DSB conversion gain. The mixer noise temperature is less than or comparable to the photon noise temperature $hf/k \approx 5.5$ K. Referred to the mixer input flange, the receiver noise temperature is ≤ 9.5 K DSB when operated with an L-band HEMT IF amplifier. Saturation measurements have been made using CW and broad-band noise sources.**

I. Introduction

SINCE THE first reports [1]–[3] of its successful use in 1979, the superconductor–insulator–superconductor (SIS) tunnel junction mixer has been recognized as the best front end for low-noise millimeter-wave receivers [4]. This is a result of the extremely low shot noise, potential conversion gain, and low local oscillator (LO) power requirement of SIS mixers. Currently, about ten SIS receivers, operating from 43 to 290 GHz, have been reported in routine use on radio telescopes around the world, although most of these have sensitivities little or no better than their main competitor, the Schottky-diode mixer receiver. We believe a major reason SIS receivers have been slow to develop their full potential is the difficulty of providing appropriate embedding impedances at the signal and image frequencies and at the higher harmonic sidebands ($n\omega_{LO} \pm \omega_{IF}$).

As a circuit element, the SIS junction is well described as a nonlinear tunneling conductance in parallel with a constant junction capacitance. In many cases the nonlinearity of the conductance is so sharp that quantum effects dominate its behavior and classical circuit analysis is inadequate to describe its operation as a mixer. A quantum theory of mixers published in 1979 by Tucker [5] gives the theoretical framework for analyzing SIS mixers. In its full form this theory is extremely complex and difficult to apply. However, if the junction capacitance is relatively large, a three-frequency approximation [6] to the full theory is justified, and this has been found to give good agreement with experiment [7], [8]. The three-frequency approximation assumes that all RF components except the LO and the upper and lower sidebands $\omega_{LO} \pm \omega_{IF}$ are short-circuited at the junction terminals. A more complete analysis of an SIS mixer using Tucker's quantum mixer theory has been attempted only for a few special cases [9], [10], which appear to indicate that the existence of higher harmonic sideband voltages reduces the conversion efficiency of the mixer.

A parameter useful in characterizing SIS junctions is the $\omega R_n C_j$ product. Here ω is the LO frequency, R_n is the normal-state junction resistance, and C_j is the junction capacitance. The earliest published results for SIS mixers indicated that a junction (or array of junctions) with an $\omega R_n C_j$ product of ~ 5 was desirable if a relatively large conversion efficiency was to be achieved [11]. More recent mixer experiments continue to support this observation. The need for such a large junction capacitance is probably to provide low embedding impedances at the LO harmonics and harmonic sidebands. To match such a highly capacitive device to a practical mount impedance requires a more complex circuit than normally used with Schottky diode mixers. If movable waveguide short circuits are used as the only matching elements, it is difficult to achieve broad-band tuning (broad-band in the sense that the junction sees nearly equal impedances in the upper and lower sidebands) and it is even more difficult to arrange for both sideband embedding impedances to be in the range necessary for low conversion loss or some gain. For this reason the mixers described in this paper have an inductive tuning element integrated with the junction (or array of junctions) to tune out the junction capacitance.

The need for an inductive tuning element integral with the SIS junction has been recognized by other workers, and several approaches have been tried with varying degrees of success. D'Addario [12] used a short supercon-

Manuscript received May 9, 1988; revised August 22, 1988. This work was supported in part by the National Science Foundation under Grant AST-8512214.

S.-K. Pan and A. R. Kerr are with the National Radio Astronomy Observatory, Charlottesville, VA 22903. NRAO is operated by Associated Universities, Inc., under contract with the National Science Foundation.

M. J. Feldman is with the Department of Electrical Engineering, University of Virginia, Charlottesville, VA 22901.

A. W. Kleinsasser, J. Stasiak, R. L. Sandstrom, and W. J. Gallagher are with the IBM Thomas J. Watson Research Center, Yorktown Heights, NY 10598.

IEEE Log Number 8825377.

0018-9480/89/0300-0580$01.00 ©1989 IEEE

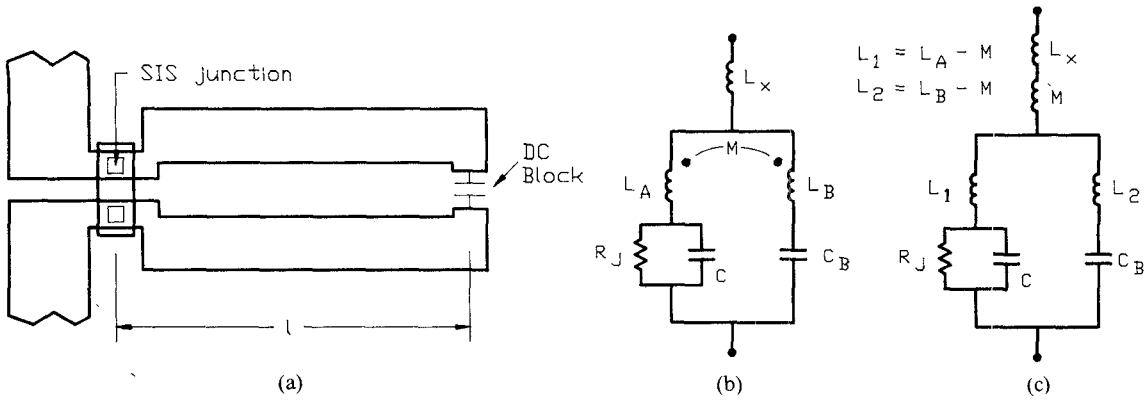

Fig. 1. (a) Simplified diagram of an inductively shunted, two-junction SIS mixer. The tuning inductor is a short parallel-strip transmission line with an RF short circuit at its right-hand end. (b) Equivalent circuit, including the mutual inductance between the array and the tuning inductor. (c) A more tractable form of the equivalent circuit.

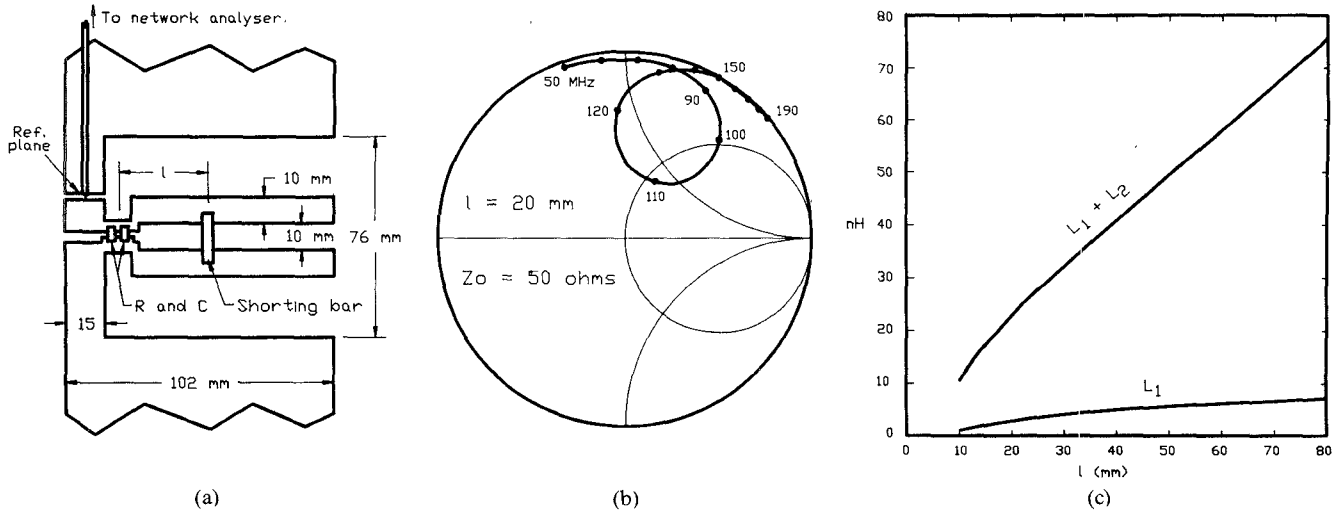

Fig. 2. (a) 1000× scale model of the inductively shunted SIS array, with the array simulated by a 98 Ω chip resistor in parallel with a 99 pF chip capacitor (these are not scaled values of the actual SIS array resistance and capacitance). (b) Measured impedance versus frequency for inductor length $l = 20$ mm. (The dominant inductive reactance is that of the external circuit, L_x in Fig. 1.) (c) L_1 and $(L_1 + L_2)$ as functions of l, deduced from measurements on the model. The variation of L_1 with l, and the departure of the $(L_1 + L_2)$ curve from a straight line, are due to the mutual inductance

ducting microstrip line terminated in a dc and IF blocking capacitor. Räisänen *et al.* [13] have used an open-circuit superconducting transmission line stub slightly longer than a quarter wavelength to provide the necessary inductance to tune out the junction capacitance. The useful frequency range of such a mixer is limited by the rapid variation of reactance with frequency for this stub. The present authors [14], [15] have used capacitor-blocked short two-wire transmission line stubs across waveguide mounted SIS arrays, a design which was unsuccessful because of the effects of the parasitic series inductance of the arrays. Woody [16] and Li *et al.* [17] have experimented with a similar approach using inductive wires across individual SIS junctions and arrays.

In the present paper we describe an SIS mixer using a series array of two Nb/oxide/PbInAu edge junctions. A broad-band tuning structure in parallel with the junctions consists of a short two-wire transmission line stub and a quarter-wave parallel-plate transmission line dc and IF block. The mixer is tunable from 85 to 116 GHz and has a double sideband (DSB) equivalent input noise temperature of $\leqslant 5.6$ K and unity DSB conversion gain at 114 GHz. In a laboratory test Dewar with a room temperature feed horn and a HEMT IF amplifier, the mixer gave an overall receiver noise temperature of 40 K DSB at midband when operated at 2.5 K. Referred to the mixer input flange, the receiver noise temperature is $\leqslant 9.5$ K DSB.

II. Design of the Inductively Shunted Junctions

In principle, a lumped inductance connected across an SIS junction could tune out the junction capacitance and allow an instantaneous RF (fractional) bandwidth of the order of $2/\omega R_n C_j$. (This result is exact if both the source resistance and the input resistance of the junction operating as a mixer are equal to R_n.) The lumped tuning inductance needs a dc block if it is not to short-circuit the junction at dc and IF. In a practical mixer, additional fixed and adjustable tuning elements may be needed to

couple efficiently between the waveguide and the junction over a reasonable tuning range. The instantaneous bandwidth is then likely to be less than in the ideal case, but can be sufficient to allow the upper and lower sidebands to be appropriately terminated.

A. Two-Wire Stub Inductor

A simplified diagram of an inductively shunted two-junction array and its equivalent circuit [14], [15] are shown in Fig. 1. The array is shunted by an electrically short two-wire transmission line stub (loop) whose inductance is determined by the length l. The inductance L_B is that of the two-wire stub. L_A is the series inductance of the array itself and should be kept small to avoid an impedance transformation between the effective junction resistance R_j and the external circuit. L_x is the inductance of the leads to the external circuit, and depends on the structure in which the inductively shunted junction is mounted (e.g., whether a waveguide, stripline, or quasi-optical mount is used). The quantity M is the mutual inductance between the stub and the array of junctions. The circuit of Fig. 1(c) is a more tractable form of Fig. 1(b), and will be referred to in the following discussion.

For the 85–116 GHz mixer described in this paper, a 1000× scale model of the inductively shunted SIS array, Fig. 2(a), was used to measure the values of L_1 and L_2 as functions of the loop length l, using a procedure similar to that described in [14] and [15]. The SIS array was simulated by a chip resistor and a chip capacitor. The two-wire transmission line stub had a movable shorting bar to adjust the length l. A ground plane was mounted below and parallel to the conductor pattern but far enough below it not to interfere with the behavior of the resonant circuit around the junction. A vector network analyzer was used to measure the impedance of the circuit. A typical measurement of impedance versus frequency is shown in Fig. 2(b). From this, the values of L_1, L_2, and $L_x + M$ for one position of the shorting bar are deduced. Fig. 2(c) shows the measured values of $(L_1 + L_2)$ and L_1 versus loop length l. The curvature of these graphs at small values of l is a result of the dependence of the mutual inductance M on l. For the mixers reported here L_1 and M are small enough not to affect the design profoundly: however, scale model measurements show that this is not always the case, particularly at high frequencies or when longer arrays are used [14], [15].

B. DC and IF Block

The dc block must be chosen to have acceptably high impedance at dc and IF while not appreciably changing the RF circuit. The use of a lumped capacitor as a dc block can be impracticable. Unless the capacitance is much greater than the array capacitance, the RF bandwidth is reduced. However, it is often difficult to fabricate a sufficiently large capacitor with electrically small dimensions because the propagation velocity in the region between two superconducting capacitor plates separated by a thin dielectric layer of high relative dielectric constant can be less than 10 percent of the free-space velocity. A second possible drawback of the simple lumped capacitor dc block is its effect on the IF circuit. If the capacitance of the block is chosen to be large compared with that of the SIS array, it may not be negligible at the IF. By using the quarter-wave stub dc block described below, these disadvantages are largely overcome. The successful use of the quarter-wave dc block in an SIS mixer was first described in [15], and it has also been used in [17].

Because of the unique properties of superconducting transmission lines [18]–[20], it is possible to make a low-loss parallel-plate quarter-wave stub with very low characteristic impedance whose physical length is many times smaller than a free-space quarter wavelength. Consider a superconducting parallel-plate transmission line whose conductors are separated by a dielectric of thickness t and relative dielectric constant ϵ_r. The London penetration depths $\lambda_{L,1}$ and $\lambda_{L,2}$ of the upper and lower conductors are assumed to be much smaller than the conductor thicknesses. Assuming TEM-mode propagation and negligible fringing at the edges of the transmission line, the phase velocity relative to that of free space is

$$\frac{v}{v_0} = \left(\frac{t}{\epsilon_r (t + \lambda_{L,1} + \lambda_{L,2})} \right)^{1/2}. \tag{1}$$

The characteristic impedance of the parallel-plate line is

$$Z_0 = \left(\frac{\mu_0}{\epsilon_r \epsilon_0} \right)^{1/2} \cdot \frac{\left(t(t + \lambda_{L,1} + \lambda_{L,2}) \right)^{1/2}}{w}. \tag{2}$$

At the IF, the capacitance of the parallel-plate line of length l_B is

$$C_B = \epsilon_r \epsilon_0 \frac{w l_B}{t}. \tag{3}$$

For a parallel-plate transmission line with a Nb lower conductor ($\lambda_{L,2} = 105$ nm) and a PbInAu upper conductor ($\lambda_{L,1} = 150$ nm) separated by Nb_2O_5 dielectric layer ($\epsilon_r = 29$) of thickness $t = 70$ nm, equation (1) gives a velocity slowing factor of 11.6. For operation at 110 GHz this requires a stub length $l_B = 59$ μm. With $w = 6$ μm, equation (2) gives $Z_0 = 1.8$ Ω, and (3) gives $C_B = 1.3$ pF.

If an open-circuit transmission line stub is a quarter wavelength long at frequency f_0, its reactance varies with frequency according to

$$X_B = Z_0 \tan\left(\frac{\pi}{2} \left(\frac{f - f_0}{f_0} \right) \right). \tag{4}$$

It follows that, with $Z_0 = 1.8$ Ω, $|X_B| < 1$ Ω over almost a 2:1 frequency range, and $|X_B| < 0.5$ Ω over a 34 percent bandwidth.

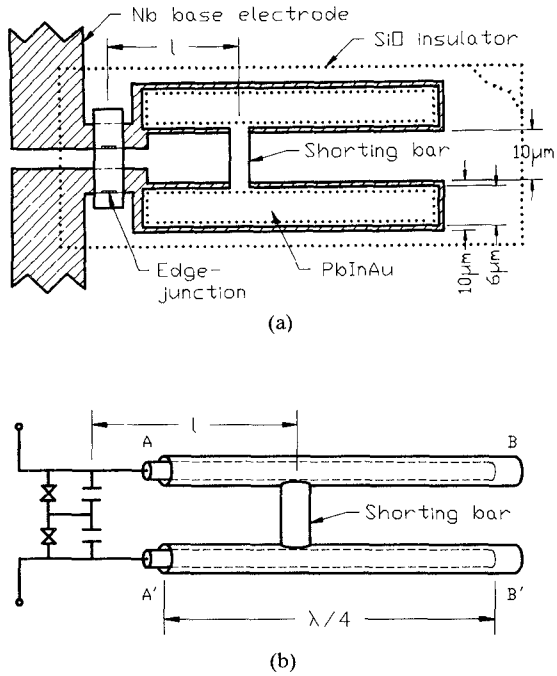

Fig. 3. (a) Diagram showing the SIS junctions and tuning circuit, approximately to scale. The tuning inductance is defined by the length *l*. The superconducting parallel-plate quarter-wave dc blocks are 11.6 times shorter than a free-space quarter wavelength. (b) Conceptual (approximate) equivalent circuit using coaxial quarter-wave stubs.

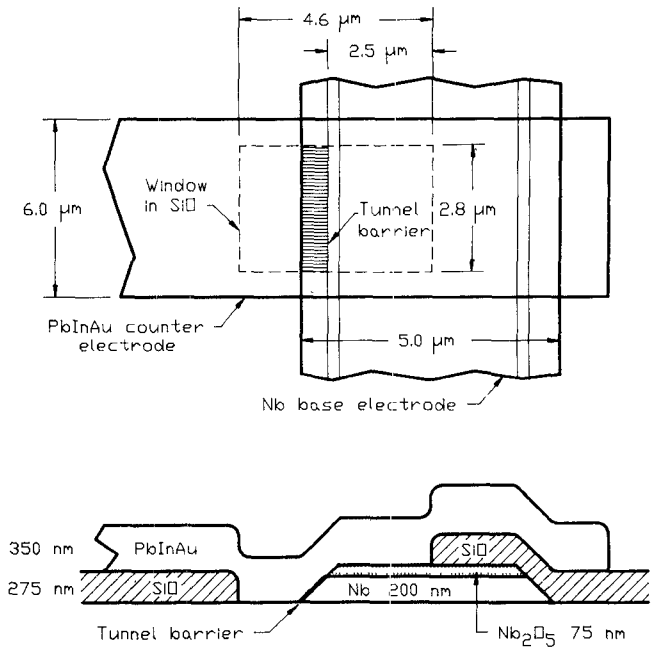

Fig. 4. Details of an edge junction as used in the present work. The electrodes are Nb and PbInAu films, and the junction is confined to the edge of the Nb film by the Nb_2O_5 layer. The junction length is defined by the SiO window.

C. Final Design

The configuration of SIS junctions, tuning inductor, and dc block used in the present work is shown in Fig. 3(a). The dc block consists of two quarter-wave parallel-plate transmission line stubs formed on top of the legs of the tuning inductor. (Two stubs are used for convenience of fabrication.) The upper conductors of the stubs are connected by the "shorting bar" whose position determines the total inductance. Operation of the circuit is most easily understood in terms of an approximate equivalent circuit, Fig. 3(b), in which the parallel-plate quarter-wave stubs are replaced with coaxial stubs. The open circuit presented to the coaxial line at B is seen as a short circuit at the other end, A. The current flowing around the tuning circuit transfers from the coaxial center conductor (Nb base electrode) across the virtual short circuit at A to the outer conductor (PbInAu upper conductor), and completes the loop via the shorting bar and the virtual short circuit at A'. While the analogy between the circuits of Fig. 3(a) and (b) is not exact, it appears to be acceptable for the case under consideration, in which the characteristic impedances and phase velocities of the two transmission line structures—the two-wire line of the tuning inductor, and the parallel-plate quarter-wave stub—are widely different. The effect of the long legs of the two-wire line and quarter-wave stubs extending well beyond the essential part of the inductive tuning loop was investigated using the 1000× scale model, and found not to be significant.

Based on our earlier experience with SIS mixers using the same waveguide mount, and on measurements on a scale model of the mount (see Section IV), a normal resistance between 50 and 100 Ω was chosen for the two-junction array, i.e., 25 to 50 Ω per junction. Choosing $\omega R_n C_j$ as discussed in Section I then completely specifies the junction parameters. The capacitance C_j includes the junction capacitance and also the overlap capacitance between the upper and lower electrodes in the vicinity of the junction. Fig. 4 shows the details of the edge junctions used in this work. For the dimensions shown in Fig. 4, the capacitance of each junction is 140 fF, and the overlap capacitance is 28 fF. For a junction with $R_n = 25$–50 Ω, this corresponds to $\omega R_n C_j = 2.6$–5.3 at 100 GHz. It will be noticed in Fig. 3(a) that both junctions in the array are formed on the lower edges of their base electrode conductors. This asymmetrical arrangement is simply an attempt to ensure uniformity of the junctions.

III. Fabrication of the Superconducting Circuit

The junctions, tuning inductor, and dc block were fabricated using the Nb/Pb-alloy technology developed at IBM [21]. The major steps in the process are:

(i) electron beam evaporation of a 230-nm-thick Nb base electrode onto a room temperature 0.015-in.-thick oxidized Si substrate;
(ii) anodization in areas defined by a photoresist pattern to form 75 nm of Nb_2O_5, leaving 200 nm of Nb;
(iii) CF_4/O_2 RF plasma etching of the Nb/Nb_2O_5 bilayer using a photomask, forming 45° edges;
(iv) definition of junction windows over the Nb edges by evaporating 275 nm of SiO and liftoff;

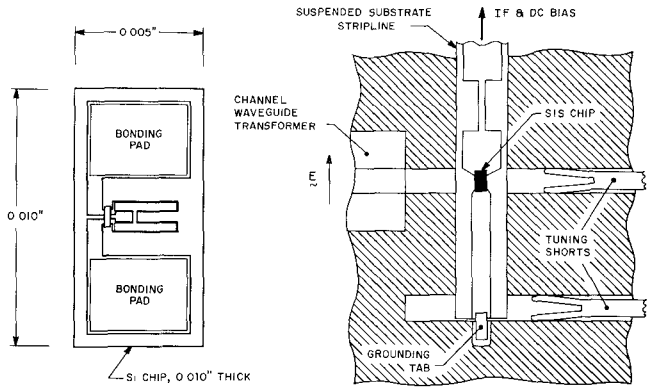

Fig. 5. Diagram of the SIS chip and a cross-sectional view of the mixer block.

(v) Ar RF plasma sputter preclean, Ar/CH_4 RF plasma growth of an NbC_xO_y diffusion barrier, Ar/O_2 RF plasma oxidation to grow the tunnel barrier, and electron beam evaporation of the PbInAu counterelectrode, all with the counterelectrode photoresist stencil in place;

(vi) Ar RF sputter preclean and evaporation of Au bonding pads.

After processing, the wafer was cut into individual 0.005 in. $\times$ 0.010 in. mixer chips which were mounted on the larger stripline circuit of the mixer.

IV. The Mixer Block

The receiver measurements were performed using the NASA/GISS type-D mixer mount [22], [23], shown in Fig. 5. This contains two adjustable tuning shorts which can provide the junctions with a wide range of embedding admittances. The SIS chip is soldered to the gold conductor pattern of the 0.023-in.-wide $\times$ 0.003-in.-thick fused quartz suspended stripline circuit, which is mounted across two quarter-height WR-10 waveguides. The upper waveguide (in Fig. 5) is connected on one side to the full-height input waveguide via a channel waveguide transformer [24] and is terminated on the other side in a sliding short circuit. The lower reduced-height waveguide is also terminated in a sliding short circuit to provide an additional degree of tuning. (The waveguide widths are actually 0.096 in., which is 0.004 in. narrower than standard WR-10, to permit operation slightly above the normal band.) The sliding short circuits are of the contacting finger type, made of gold-plated beryllium copper.

The SIS chip is mounted on the larger suspended stripline circuit using Alpha B20E2 solder [25] (96°C melting point) and Supersafe #30 flux [26]. The PbInAu conductor pattern on the chip was masked with photoresist during soldering to prevent the flux from attacking it.

An equivalent circuit of the mount is shown in Fig. 6(a). The choice of this form for the equivalent circuit is based on the work of Eisenhart and Khan [27], [28], from which we are able to identify the circuit reactances with energy storage in particular groups of evanescent waveguide modes excited by particular parts of the mount. The inductances

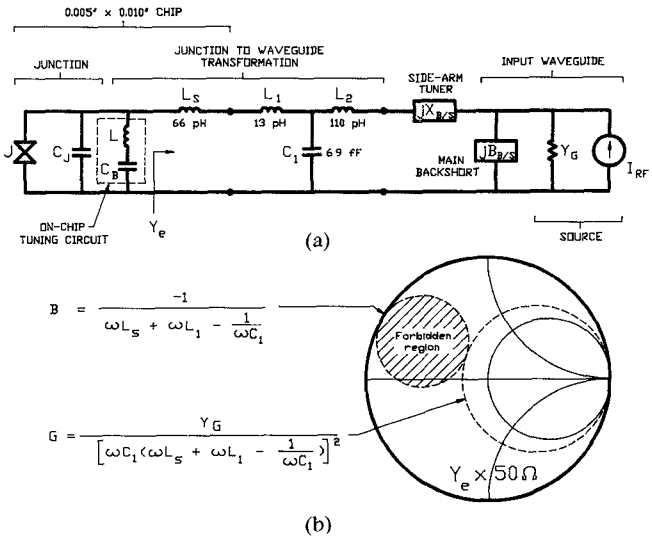

Fig. 6. (a) Equivalent circuit of the mixer. (b) Smith chart (admittance coordinates) showing the available range of embedding admittances, Y_e in (a), at 100 GHz. Embedding admittances lying within the shaded circle cannot be obtained with this circuit.

L_S, L_1, and L_2 are associated with the evanescent TE_{m0} modes ($m > 1$), while the capacitance C_1 is associated with the evanescent TE_{mn} and TM_{mn} modes. This choice of equivalent circuit results in elements that are not strongly frequency dependent, and allows a more intuitive understanding of the mount. In principle, the equivalent circuit element values could be derived from an Eisenhart and Khan type of analysis. However, in the present work we used a 40$\times$ scale model of the mount and a 1000$\times$ scale model of the SIS chip to measure the element values [23]; typical values are indicated in Fig. 6(a). The tuning range of this mount at 100 GHz is indicated on the Smith chart in Fig. 6(b).

V. Test Receiver

The properties of the mixer were evaluated using a test receiver designed for determining the conversion loss and noise temperature entirely from noise measurements. A diagram of the receiver is shown in Fig. 7. The noise temperature of the whole receiver is measured by the Y-factor method with hot (room temperature) and cold (77 K) loads in front of the feed horn. Using the IF switch, the internal IF hot (20 K) and cold (4 K) loads allow the noise temperature of the IF section to be determined accurately. The switch also enables the IF power reflection coefficient of the mixer to be measured by injecting an external IF test signal through the circulator while switching between the mixer and the short circuit reference. A 20 dB directional coupler allows a calibration signal to be injected directly into the IF amplifier. More complete details of the measurement procedure are given in Section VI. The test receiver has certain features in common with that described in [29], in which the mixer is terminated in a heatable RF cold load inside the cryostat—an arrangement which allows very precise measurement of the mixer noise temperature. By using an input waveguide from

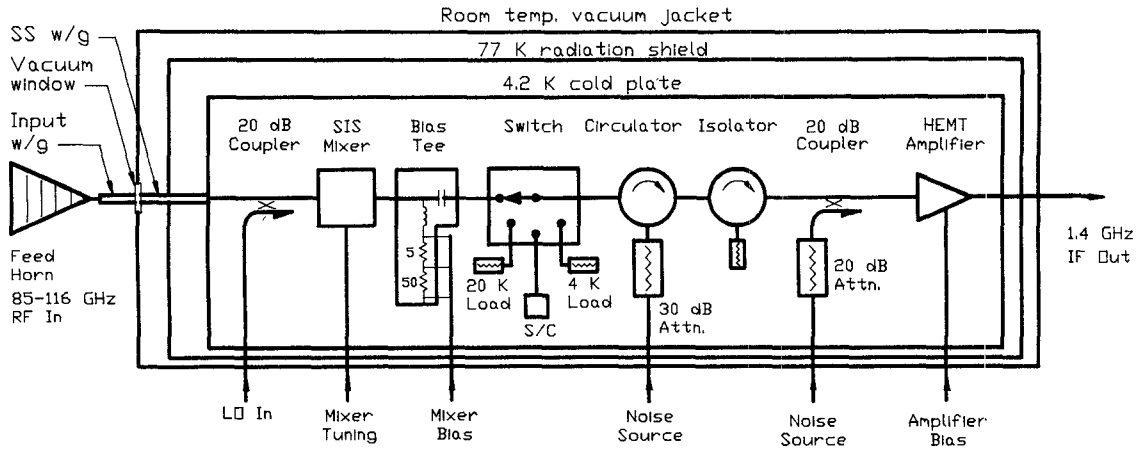

Fig. 7. Block diagram of the laboratory test receiver.

outside the cryostat, our receiver not only is of a configuration useful for radio astronomy [23], but is more suitable for some RF measurements on the mixer, e.g., measurement of saturation using broad-band noise. The price we pay is a greater uncertainty in the mixer noise temperature.

The receiver is housed in a vacuum cryostat [30] containing a liquid-helium-cooled cold plate and a liquid-nitrogen-cooled radiation shield. The pyramidal feed horn is coupled to the mixer through a section of coin silver waveguide, a vacuum window, a stainless-steel waveguide, and a 20 dB branch line LO coupler which is well connected thermally to the 4.2 K cold plate.

The stainless-steel waveguide is 2.4 in. long and is attached to a 77 K heat sink 0.7 in. from its room temperature end. It is copper plated on the inside [31] to a thickness of 0.6 μm, which reduces its midband loss to $\sim$ 0.10 dB/in. at room temperature.

The vacuum window is a low reflection PTFE/fused quartz/PTFE sandwich epoxied into a short WR-10 waveguide section. The quartz and Teflon layer thicknesses are, respectively, 0.0159 in. and 0.0222 in. The surface of the Teflon is chemically treated [32] to achieve good adhesion with Eccobond 45 [33]. The return loss of the window is $>$ 25 dB from 110 to 116 GHz and $>$15 dB from 90 to 116 GHz.

The biasing scheme for the mixer is described in [34]. The bias voltage for the mixer is developed across a cold 50 Ω resistor in the bias T by a current source external to the Dewar. Two servo loops are used: the inner one controls the current source to maintain a constant voltage across the junction, while the outer loop adjusts the LO drive level to maintain a preset junction current. All bias and monitor connections enter the Dewar through four-element 10 kHz low-pass feed-through filters.

The single-pole four-throw coaxial IF switch [35] was modified to prevent static charging of the moving contact bars during switching. Static charge generation by the motion of the contact bars against PTFE guide pins was found to occur intermittently in all the commercial switches we tested, and was responsible for the destruction of many of our early Pb alloy SIS junctions. To avoid this, a grounded 10 kΩ chip resistor was connected by a 0.25-in.-long, 0.002-in.-diameter beryllium copper spring wire to each moving contact bar. The wires, mounted in channels machined in the base plate of the switch, form short high-impedance transmission lines, and are sufficiently flexible not to restrict the movement of the contact bars. The return loss of the modified switch was $>$ 26 dB over 1–2 GHz, which is comparable to that of the unmodified switch.

The circulator and the isolator were designed for cryogenic operation [36], and have a 20 dB isolation bandwidth of $\sim$ 400 MHz. The 20 dB directional coupler is of the air dielectric stripline type [37], and the only modification necessary was to drill a small breather hole in the lid.

The cold attenuators [38] have nichrome film resistive elements, well heat sunk by an alumina substrate held in the attenuator barrel by firm spring clips. The conductive rubber contact buttons between the connector center conductors and the edge of the substrate were replaced by bellows contacts [39].

The 4 K and 20 K loads were commercial medium power terminations [40] with nichrome film resistors well connected thermally to copper housings. The heated (20 K) load was connected to the switch by a 2.0-in.-long, 0.085-in.-diameter stainless-steel coaxial cable whose loss (0.21 dB at 15 K) requires a small correction (0.27 K) to the effective hot load temperature referred to the switch.

The noise temperature of the *L*-band IF section, measured by switching between the internal hot and cold loads, is 3.2 K at 4.2 K physical temperature, and 2.9 K at 2.5 K physical temperature. (At 1.4 GHz the HEMT IF amplifier itself [41] has a noise temperature of 1.9 K at physical temperatures of both 4.2 K and 2.5 K.) An IF bandwidth of 50 MHz at 1.4 GHz was used for the measurements reported here.

VI. Measurement Method

As generally used in the microwave community, *noise temperature* is actually a convenient way of expressing *noise power* per unit bandwidth. At the temperatures and frequencies normally encountered in microwave engineer-

ing, the noise power available from a resistor or load at physical temperature T_{phys} is given by the Rayleigh–Jeans law: $P = kT_{\text{phys}}B$. At high frequency and low temperature it is necessary to use the more general expression of Callen and Welton [42] for the radiated power to take account of the departure of the blackbody radiation curve from the Rayleigh–Jeans law:

$$P = \frac{hfB}{2} \coth \frac{hf}{2kT_{\text{phys}}}. \tag{5}$$

The Callen and Welton expression follows the Planck radiation law with the addition of the zero-point fluctuation power $hfB/2$. Throughout this paper, physical temperature T_{phys} is converted to available noise power according to (5), which is then represented by radiation temperature $T' = P/kB$. Likewise, all other noise powers are represented by temperatures according to $T = P/kB$. In fact, the differences in the noise temperatures given by the Rayleigh–Jeans law and the Callen and Welton law at 114 GHz are 0.9 K at $T_{\text{phys}} = 2.5$ K and 0.6 K at $T_{\text{phys}} = 4.2$ K, but only 0.03 K at $T_{\text{phys}} = 77$ K. Note that, in using the Callen and Welton law, the incident signal power calculated at the input of the mixer includes the zero-point fluctuations; thus, a double sideband mixer can in theory have a noise temperature of zero without violating the requirements of the uncertainty principle. For a further discussion of these issues, see [43].

The overall receiver noise temperature T_r is measured by the Y-factor method using room-temperature and 77 K blackbodies in front of the room-temperature feed horn. If the insertion loss from the input of the horn to the mixer is L_t and the effective noise temperature of this loss is T_t referred to the input of the receiver, then the intrinsic receiver noise temperature T_r', referred to the input of mixer, is given by

$$T_r = L_t T_r' + T_t. \tag{6}$$

T_r' is related to the conversion loss L_c and the noise temperature T_m of the mixer through

$$T_r' = T_m + T_{\text{LO}} + L_c\left(T_{\text{IF}} + |\Gamma_0|^2 T_b\right) \tag{7}$$

where T_{LO} represents noise from the LO system injected through the LO coupler, T_{IF} is the effective input noise temperature of the IF system, and $|\Gamma_0|^2 T_b$ is the IF noise reflected by the mixer from the termination at temperature T_b on the IF input circulator. The receiver can be tuned for either single sideband or double sideband response, and (6) and (7) are valid in either case provided T_r, T_m, and L_c are all either single sideband or double sideband quantities.

Since T_r and T_{IF} are linearly related, measurement of T_r for two known values of T_{IF} enables T_m and L_c to be determined provided the constants L_t, T_t, T_{LO}, and $|\Gamma_0|^2 T_b$ are known. Our procedure is a variation of that described by Trambarulo and Berger [44] and is chosen because of its relative insensitivity to drift in the overall system gain during measurements. In the test receiver, T_{IF} can be changed by injecting IF noise through the directional coupler toward the IF amplifier. The effective T_{IF}, measured at the input of the coaxial switch, is determined from a Y-factor measurement by switching the input of the IF amplifier between the 20 K heated load and the 4.2 K load. Using this method, T_{IF} can be measured with an accuracy better than 0.5 K. The factors affecting the accuracy of these measurements are discussed in Section VII.

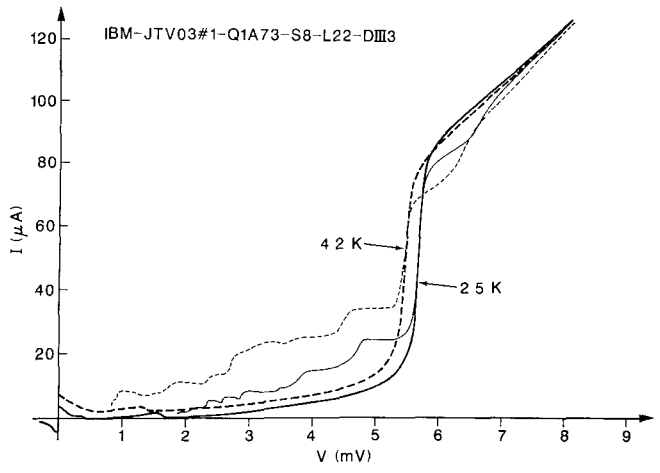

Fig. 8. Typical dc $I-V$ curves with and without LO power applied to the mixer. These curves were measured at 4.2 K (---) and 2.5 K (———) with the LO at 114 GHz. The mixer tuning and LO power were adjusted to give a horizontal step below the gap voltage.

The test receiver allows the mismatch at the IF port of the mixer to be determined. Depending on the IF switch setting, an IF signal (CW or noise) can be injected through the circulator towards either the mixer's output port or the short-circuit termination. The power reflection coefficient $|\Gamma_0^2|$ at the output of the mixer is obtained by comparing the power reflected in these two cases. The accuracy of this measurement is primarily limited by the directivity of the circulator.

VII. Results

The $I-V$ curves of a typical pair of junctions, measured at 2.5 K and 4.2 K, with and without LO power applied, are shown in Fig. 8. It is significant that, despite the relatively soft (unpumped) $I-V$ curve, we were easily able to tune the mixer for horizontal steps on the pumped $I-V$ curve. This was the first indication that the tuning circuit was performing properly.

Fig. 9 shows the DSB noise temperature of the receiver at 4.2 K as a function of frequency. Also shown are several SSB results for which the mixer was tuned to reject the image by ≥ 20 dB, and some results with the receiver cooled to 2.5 K by reducing the pressure in the liquid helium tank. These results are raw receiver noise temperatures measured at the room temperature horn and contain no corrections for the losses in the horn or input waveguide.

As indicated by (6) and (7), the receiver noise temperature T_r displayed in Fig. 9 contains contributions from the mixer noise, the noise in the IF section, and noise due to

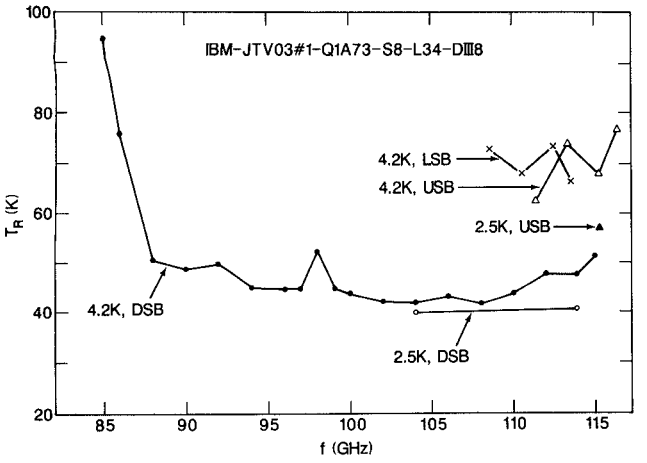

Fig. 9. Overall receiver noise temperature as a function of frequency. Measurements were made at 2.5 K and 4.2 K, and with the mixer tuned for DSB operation or SSB operation in the upper of lower sideband (USB or LSB) as indicated. For all SSB measurements the image response was ≥ 20 dB below the signal response. At 2.5 K the IF noise temperature was 2.9 K. Typical LO power was 20 nW referred to the input flange of the mixer. The noise temperature scale indicates T_r (DSB) for DSB results and T_r (SSB) for SSB results.

TABLE I
NOISE BUDGET FOR MIXER DIII8 IN LABORATORY TEST RECEIVER

	L	T_{phys}	T_n	Contrib. to T_r	T_r DSB
Horn	0.10 dB	298	6.9	6.9	40.6
W/G	0.15 dB	298	10.5	10.7	32.9
Window	0.10 dB	298	6.9	7.4	21.7
SS w/g #1	0.07 dB	200	3.2	3.5	14.7
SS w/g #2	0.11 dB	50	1.3	1.4	11.0
LO coupler	0.07 dB	2.5	0.1	0.1	9.5
Coupled noise	—	—	3.0	3.4	9.3
Mixer & Bias-T	0.10 dB	—	3.4	3.9	6.3
Refl. IF noise	—	2.5	0.4	0.4	2.8
IF System	—	—	2.4	2.8	2.4

The receiver is tuned for DSB operation with $f_{\text{LO}} = 114$ GHz at a cold-plate temperature of 2.5 K. The IF VSWR is 2.3. The loss (L) and effective physical temperatures (T_{phys}) of the input components are here set to their expected values, either measured or estimated. T_n is the equivalent input noise temperature of the individual components. T_r is the DSB receiver noise temperature referred to the input of each component. The value of the mixer noise temperature (3.4 K) was deduced from the measured overall receiver noise temperature (40.6 K).

the RF components ahead of the mixer. In order to deduce the noise temperature of the mixer itself from T_r, the other noise contributions must be accurately known. In our receiver, the noise from the RF components ahead of the mixer is by far the dominant part of T_r. It is therefore very important to determine T_l and L_l in (7) as precisely as possible.

We chose two LO frequencies at which to analyze the receiver performance, 104 GHz, corresponding to the best overall receiver noise temperature, and 114 GHz, which is of special interest to astronomers as the 115.3 GHz CO line then falls in the upper sideband.

As the waveguide loss could not be measured directly with the Dewar cold, the following approach was taken: First, the loss was measured directly at room temperature. A short circuit was then connected at the end of the waveguide, and swept return loss measurements made using a reflectometer, first at room temperature, then with the Dewar cold. It is well known that the finite directivity of reflectometers severely limits the accuracy of round-trip loss measurements; however, by combining the observed *change* in loss on cooling (obtained from the reflectometer measurements) with the directly measured insertion loss at room temperature, we are able to obtain an accurate value for the waveguide loss. In the present case $L_{\text{wg}} = 0.50 \pm 0.10$ dB near 104 GHz and 0.50 ± 0.06 dB near 114 GHz (this is for the input waveguide, vacuum window, stainless-steel waveguide, and LO coupler). The theoretical value was used for the loss of the horn. This gives a total input loss $L_l = 0.60 \pm 0.13$ dB near 104 GHz and 0.60 ± 0.09 dB near 114 GHz.

We determined the effective noise temperature T_l of the waveguide components ahead of the mixer in two ways:

(i) By measuring or estimating the loss and physical temperature of the various waveguide sections, and thereby deducing T_l.

(ii) By measuring the noise radiated out of the input flange when the cold end of the waveguide is terminated in a cold load. From this, it is possible to place limits on T_l.

Method (i): Because of the strong temperature dependence of the thermal conductivity of stainless steel, and the unknown thermal conductivity of the 0.6 μm electroplated copper layer inside the waveguide (which carries a significant fraction of the heat flow), the temperature distribution along the waveguide cannot be calculated precisely. Likewise, because we do not know the thermal dependence of the RF loss of the copper plating, it is not possible to determine the distribution of loss along the waveguide. However, we can make reliable estimates of the upper and lower bounds of these quantities, and thereby arrive at corresponding limits for T_l. At 114 GHz, for example, we obtain $23.4 \leq T_l \leq 39.0$ K.

Table I shows a typical noise analysis with the receiver tuned for DSB operation at 114 GHz. The primary measured quantity is the overall receiver noise temperature (40.6 K). With the expected values of the loss and noise temperatures of the input components, we deduce the mixer noise temperature $T_m = 3.4$ K. Allowing the estimated values of the component losses and effective physical temperatures to vary over their expected ranges gives $-5.5 \leq T_m \leq 11.3$ K. Since T_m cannot be negative, we can say that $T_m \leq 11.3$ K. The corresponding receiver noise temperature at the input of the mixer is $2.9 \leq T_r \leq 14.2$ K DSB, or $3.9 \leq T_r \leq 15.4$ K DSB at the LO coupler.

Method (ii): If the loss of the input waveguide components is small, the thermal noise radiated from the hot and cold ends is nearly the same. By measuring the noise radiated out of the input flange when the cold end of the waveguide is terminated in a cold load, it is possible to put close limits on the power radiated from the cold end. We used a Schottky-diode mixer receiver with an input isolator to measure the equivalent noise temperature T_e at the

TABLE II
TYPICAL MIXER CHARACTERISTICS

Mixer	Temp.	$R_{n,a}$	l	f_{LO}	$\omega R_n C_j$	SSB/DSB	L_c	IF VSWR	T_m min	T_m max
DIII5	4.2 K	60 Ω	27 μm	114 GHz	3.6	DSB	1 9 dB	2.1	−11.5	7.5 K
DIII5	4.2 K	60 Ω	27 μm	114 GHz	3.6	SSB	5.8 dB	1.5	−2.1	21.1 K
DIII8	4.2 K	64 Ω	34 μm	114 GHz	3.9	DSB	2.7 dB	2.2	−10.3	8.4 K
DIII8	4.2 K	64 Ω	34 μm	114 GHz	3.9	SSB	6.1 dB	1.8	−2.7	19.0 K
DIII8	2.5 K	64 Ω	34 μm	114 GHz	3.9	DSB	0 1 dB	2.3	−12.1	5.6 K
DIII8	2.5 K	64 Ω	34 μm	104 GHz	3.5	DSB	−0.1 dB	4.9	−12.4	13.4 K

$R_{n,a}$ is the normal resistance of the two-junction array, and l is the length of the tuning inductor as defined in Fig 3(a) L_c and T_m are the conversion loss and input noise temperature of the mixer, SSB or DSB as indicated. L_c is the transducer conversion loss; i.e., it is not corrected for input or output mismatch. The upper and lower limits given for T_m are those predicted by the worst-case error analysis (method (ii)) described in the text.

room-temperature waveguide flange. The return loss was also measured using a swept reflectometer. T_e is composed of the thermal radiation $T_{x,h}$ of the waveguide, thermal radiation T_b^r from the cold termination, and reflected noise from the room-temperature (T_a) input isolator of the Schottky receiver. Hence

$$T_{x,h} = T_e - |\Gamma_{in}|^2 T_a - \frac{T_b^r}{L_{wg}}. \tag{8}$$

As an example of this method, with the Schottky receiver operating at an LO frequency of 114 GHz, we measured an effective noise temperature at the input waveguide flange $29.1 \leqslant T_e \leqslant 36.9$ K and $22.9 \leqslant T_{x,h} \leqslant 32.5$ K. Using the method described in the Appendix, with input waveguide loss $L_{wg} = 0.50 \pm 0.06$ dB (see above), the thermal noise radiated from the cold end of the waveguide is $22.4 \leqslant T_{x,c} \leqslant 32.1$ K. Referring this to the input of the feed horn gives $30.0 \leqslant T_i \leqslant 46.7$ K. For the example discussed above and in Table I, with the receiver operating in DSB mode at 114 GHz and 2.5 K, method (ii) gives $-12.1 \leqslant T_m \leqslant 5.6$ K, or, since T_m cannot be negative, $T_m \leqslant 5.6$ K DSB. The corresponding receiver noise temperature at the input of the mixer is $2.9 \leqslant T_r \leqslant 9.5$ K DSB, and at the LO coupler $3.9 \leqslant T_r \leqslant 12.8$ K DSB.

The two methods for deducing the mixer noise temperature from the overall receiver measurements are in reasonable agreement and give about the same absolute uncertainty in T_m.

The accuracy of the mixer conversion loss deduced from overall receiver noise measurements using (6) and (7) depends on the uncertainty of the loss ahead of the mixer and the calibration of the IF noise temperature. For the present work we estimate an uncertainty in the conversion loss of ±0.2 dB.

Table II gives typical mixer characteristics, deduced from overall receiver measurements, for different tuning conditions (SSB or DSB, and inductor length l), physical temperatures, and LO frequencies. The maximum and minimum values of T_m given in the table are based on a worst-case error analysis in which all errors are additive. No corrections for impedance mismatches at the input and output of the mixer have been made to these results (i.e., L_c is the transducer conversion loss).

TABLE III
SATURATION CHARACTERISTICS

SSB/DSB	P_{LO}	L_c	P_{1dB} CW*	P_{1dB} Theory	T_{1dB} Noise*	Implied BW
DSB	22 nW	1.9 dB	1.6 nW	1 6 nW	3810 K	30 GHz
SSB	37 nW	5.8 dB	2.9 nW	2 0 nW	4260 K	34 GHz

Mixer DIII5 at 4.2 K with $f_{LO} = 114$ GHz.
* = measured at receiver input.

The output VSWR's of the mixers are also given in Table II. With the mixer tuned for single sideband operation, the IF VSWR was normally close to 2, while for double sideband operation it was usually in the range 2–5.

VIII. SATURATION

Saturation by CW or noise input signals generally occurs at much lower powers in SIS mixers than in other practical microwave devices, and for this reason it is particularly important to determine the saturation characteristics of SIS receivers. Table III gives the input signal levels necessary to produce 1 dB gain compression using both CW and broad-band noise sources. Note that the CW 1 dB gain compression point is roughly one tenth of the LO power. A broad-band RF noise source (gas noise tube) used as the input signal gives 1 dB mixer saturation for temperatures of 3800 K and 4300 K for DSB and SSB operation, respectively. The saturation measurements will be discussed in an ensuing publication [45].

Saturation in SIS mixers usually results from modulation of the gain by the IF output voltage, and this is the basis for the analysis of saturation [46]–[48] used to calculate the theoretical saturation powers quoted in Table III. It is seen that the measured CW saturation powers are in reasonable agreement with theory. In addition, the saturation curve, i.e., the dependence of the receiver output power upon the signal power, agrees quite precisely with the theoretical expression, for both CW and noise signals [45].

In the case of saturation by broad-band noise, a comparison with the theory requires a knowledge of the effective noise bandwidth. This depends upon the mixer gain at all RF frequencies from which down-converted noise contributes to the output voltage, and upon the mixer output

impedance and IF load impedance over the corresponding range of intermediate frequencies [47]. This IF range is likely to be far wider than the nominal IF band—in the present case, tens of GHz compared with 500 MHz. The complexity of the RF circuit, together with the lack of information about the IF circuit beyond its nominal band (especially the isolators), puts a computation of the theoretical noise saturation level beyond the scope of the present work. Instead, we simply calculate the "implied bandwidth," which is the effective noise bandwidth that would be required for the thermal noise saturation power, $P = kT_{1dB}B$, to equal the theoretically calculated P_{1dB}. The implied noise bandwidths for the DSB and SSB cases, listed in Table III, are approximately equal. Although this may seem surprising, it is explained by an examination of the embedding impedance as a function of frequency using the equivalent circuit of the mount (Fig. 6(a)). In the SSB mode, image rejection is produced only over a relatively narrow band compared with the full RF bandwidth. In DSB operation the image rejection band is simply moved beyond the nominal upper and lower sidebands, but the general character of the embedding impedance versus frequency is not greatly changed. It is interesting to note that, for this experiment, the implied bandwidth of this receiver is about one half of the "Q bandwidth" (63 GHz), obtained by dividing twice the operating frequency by the $\omega R_n C_j$ product of the junctions.

The relatively low saturation power of the SIS mixer compared to conventional semiconductor mixers may restrict its use for some applications. The present receiver is acceptable in this respect for most astronomical observations; however, its 1 dB saturation temperature (3800 K) will not allow observation of the sun (6000 K) without special calibration procedures. As the saturation power (or temperature) of an SIS mixer is proportional to the square of the number of junctions [11], an immediate solution to this problem is to use arrays of more than two junctions.

IX. Discussion

Despite the relatively soft $I-V$ curve of the two-junction arrays used in these mixers, low mixer noise temperature and conversion loss were achieved, and the receiver tuned easily over 85–116 GHz. The rapid increase in receiver noise temperature below 88 GHz is due to the cutoff of the channel waveguide transformer [24] in the mixer block.

The lowest mixer noise temperature, $T_m \leqslant 5.6$ K DSB, is less than or comparable to the photon noise temperature hf/k (5.5 K at 114 GHz). Referred to the mixer input flange, the receiver noise temperature $T_r \leqslant 9.5$ K DSB. The minimum theoretical noise temperature for mixer receivers is limited by the Heisenberg uncertainty principle [4], [43]. For a receiver which responds only to a single sideband, the receiver must contribute an equivalent input noise temperature of at least $hf/2k$, i.e., half the photon noise temperature. For a double sideband receiver, the requirements of the uncertainty principle are met by the zero-point fluctuation temperature $hf/2k$ in each of the two sidebands, and a minimum DSB receiver noise temperature of zero is possible.

From the dc $I-V$ curve of the two-junction array it is possible to predict the expected mixer characteristics using Tucker's theory in its three-frequency form [4]. Knowing the bias voltage and dc current in the pumped mixer and the IF load impedance (50 Ω), we examined the performance of the mixer as a function of RF source admittance. At 114 GHz, a source admittance of $0.04 + j0.02$ should give $T_m = 5.5$ K DSB, $L = -0.4$ dB (i.e., a small gain), and an IF output impedance of 130 Ω (VSWR = 2.6), which are close to our measured values: $T_m \leqslant 5.6$ K, $L_c = 0.1$ dB, and IF VSWR = 2.3. Adjusting the source admittance and LO power to minimize T_m the theory predicts $T_{m,\min} \approx 4.5$ K with $L_c \approx -3$ dB and an output impedance of 550 Ω. While these predictions assume identical signal and image terminations, the 2.8 GHz frequency difference between the sidebands generally results in somewhat unequal terminations. This is likely to account for the small differences between the best theoretical and observed values of noise temperature and conversion loss.

For the test receiver described here, the minimum overall receiver noise temperature, 40 K, was limited primarily by the loss of the warm input waveguide components. If these components were replaced by a cold feed horn mounted directly on the LO coupler and a room-temperature vacuum window, as is commonly done in cryogenic radio astronomy receivers, the receiver noise temperature could be substantially reduced. A further improvement could be obtained by removing several lossy IF components—the switch, isolator, and directional coupler. With these improvements, and assuming the loss of a cold feed horn to be 0.1 dB, the room-temperature vacuum window 0.1 dB, an IF noise temperature of 2.2 K, and a mixer noise temperature of 5.6 K DSB, an overall receiver noise temperature of 18 K DSB should be achievable (of which 7 K is contributed by the room-temperature window). The useful bandwidth of the receiver is limited by the IF components. The better amplifiers of the type used in this work have a noise temperature variation of less than a factor of 2 over more than 500 MHz, which is comparable to the bandwidth of the circulator and isolator.

We believe that integrated tuning circuits similar to the one described here or to the higher frequency variations described in [15] will allow future SIS receivers to approach their full potential as ultra-low-noise front ends in future millimeter- and submillimeter-wavelength systems.

Appendix
Noise Contribution of Dewar Input Waveguide

The major source of measurement error in testing cryogenic low-noise mixers and amplifiers is often the uncertainty in the noise contribution of the input waveguide (or cable). While it may be possible to measure the loss of this waveguide quite accurately at the operating temperature, the temperature distribution along its length cannot usually be determined with any certainty. One could, of course, calculate the limits on the noise contribution of the waveguide in the extreme cases in which all the loss is assumed to be either at the hot end of the waveguide or at the cold end. In this Appendix we present a technique

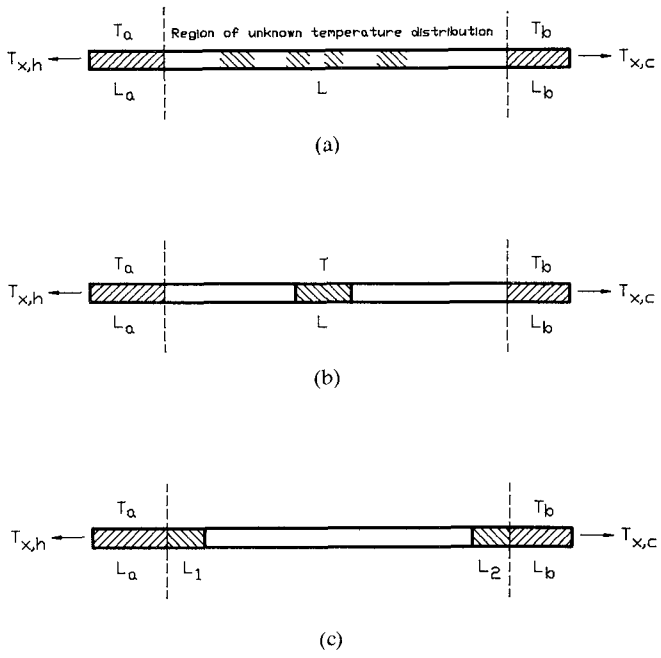

Fig. 10. (a) Input waveguide, with loss L_a and L_b at the ends at known temperatures T_a and T_b, and loss L in the central region of unknown temperature distribution. In (b) the loss L in the central region is assumed all to be at temperature T, where T is chosen to give the measured value of $T_{x,h}$. This gives the highest possible value of $T_{x,c}$. In (c) the loss L in the central region is assumed divided into two parts, L_1 at temperature T_a and L_2 at T_b, where L_1 and L_2 are chosen to give the measured value of $T_{x,h}$. This gives the lowest possible value of $T_{x,c}$.

which narrows these limits by measuring the noise T_e emitted from the hot end of the waveguide when the cold end is terminated in a cold matched load. It is assumed that the thermal noise $T_{x,h}$ originating in the waveguide loss and emitted from the hot end has been deduced from T_e using measured values of the input return loss, waveguide loss, and the physical temperature of the cold load, as described in Section VII.

Let $T_{x,c}$ denote the thermal noise, originating from the waveguide loss, emerging from the cold end of the waveguide. It is the purpose of this Appendix to determine the upper and lower limits on $T_{x,c}$, given $T_{x,h}$ but not knowing the temperature distribution along the lossy waveguide.

Assume the ends of the waveguide are at temperatures T_a (room temperature) and T_b (the bath temperature). Of the total loss of the waveguide L_{wg} (measured with the Dewar cold), let L_a be at temperature T_a, and L_b at T_b. The remaining loss, $L = L_{\text{wg}}/L_aL_b$, has an unknown temperature distribution. This situation is depicted in Fig. 10(a). The temperature distributions which give maximum and minimum values of $T_{x,c}$ for a given value of $T_{x,h}$ are shown, respectively, in Fig. 10(b) and (c).

Referring to Fig. 10(b) (the configuration giving the maximum $T_{x,c}$),

$$T_{x,h} = T_a\left(1-\frac{1}{L_a}\right)+T\frac{1}{L_a}\left(1-\frac{1}{L}\right)+T_b\frac{1}{LL_a}\left(1-\frac{1}{L_b}\right) \tag{A1}$$

and

$$T_{x,c}|_{\max} = T_b\left(1-\frac{1}{L_b}\right)+T\frac{1}{L_b}\left(1-\frac{1}{L}\right)+T_a\frac{1}{LL_b}\left(1-\frac{1}{L_a}\right). \tag{A2}$$

It follows that

$$T_{x,c}|_{\max} = \frac{L_a}{L_b}T_{x,h}-\frac{L_a}{L_b}\left(1-\frac{L_b}{L_{\text{wg}}}\right)T_a\left(1-\frac{1}{L_a}\right)+\left(1-\frac{L_a}{L_{\text{wg}}}\right)T_b\left(1-\frac{1}{L_b}\right). \tag{A3}$$

This is the largest possible value of $T_{x,c}$. The smallest possible value occurs when the loss L is divided between the hot and cold ends of the waveguide. Referring to Fig. 10(c), $L_{\text{wg}} = L_1L_2L_aL_b$, where only L_a and L_b are known. Then

$$T_{x,h} = T_a\left(1-\frac{1}{L_1L_a}\right)+\frac{1}{L_1L_a}T_b\left(1-\frac{1}{L_2L_b}\right) \tag{A4}$$

and

$$T_{x,c}|_{\min} = T_b\left(1-\frac{1}{L_2L_b}\right)+\frac{1}{L_2L_b}T_a\left(1-\frac{1}{L_1L_a}\right). \tag{A5}$$

It follows that

$$T_{x,c}|_{\min} = \frac{(T_a-T_b)^2}{L_{\text{wg}}(T_a-T_{x,h})-T_b}+T_b-T_a\frac{1}{L_{\text{wg}}}. \tag{A6}$$

This is the smallest possible value of $T_{x,c}$.

ACKNOWLEDGMENT

The authors wish to thank B. Bumble, M. Crawford, N. Horner, and C. Jessen for their expert assistance in fabricating the mixers and test equipment.

REFERENCES

[1] P. L. Richards, T. M. Shen, R. E. Harris, and F L. Lloyd, "Quasiparticle heterodyne mixing in SIS tunnel junctions," *Appl. Phys. Lett.*, vol. 34, no. 5, pp. 345–347, 1 Mar. 1979.

[2] G. J. Dolan, T. G. Phillips, and D. P. Woody, "Low-noise 115-GHz mixing in superconducting oxide-barrier tunnel junctions," *Appl. Phys Lett*, vol 34, no. 5, pp. 347–349, 1 Mar. 1979.

[3] S Rudner and T. Claeson, "Arrays of superconducting tunnel junctions as low noise 10-GHz mixers," *Appl. Phys Lett.*, vol. 34, no. 10, pp. 711–713, 15 May 1979.

[4] J R. Tucker and M. J Feldman, "Quantum detection at millimeter wavelengths," *Rev. Mod Phys.*, vol. 57, no. 4, pp. 1055–1113, Oct. 1985.

[5] J. R. Tucker, "Quantum limited detection in tunnel junction mixers," *IEEE J. Quantum Electron.*, vol. QE-15, pp. 1234–1258, Nov. 1979.

[6] J. R. Tucker, "Predicted conversion gain in superconductor–insulator–superconductor quasi-particle mixers," *Appl. Phys. Lett.*, vol. 36, pp. 477–479, 15 Mar. 1980.

[7] T. G. Phillips and G. J. Dolan, "SIS mixers," *Physica*, vol 109& 110B, pp. 2010–2019, July 1982.

[8] M. J. Feldman, S.-K. Pan, A. R. Kerr and A. Davidson, "SIS mixer analysis using a scale model," *IEEE Trans. Magn.*, vol. MAG-19, pp. 494–497, May 1983.

[9] P. L. Richards and T.-M Shen, "Superconductive devices for millimeter-wave detection, mixing, and amplification," *IEEE Trans. Electron Devices*, vol. ED-27, pp. 1909–1920, Oct. 1980.
[10] R. G. Hicks, M. J. Feldman, and A. R. Kerr, "A general numerical analysis of the superconducting quasiparticle mixer," *IEEE Trans. Magn.* vol. MAG-21, pp. 208–211, Mar. 1985.
[11] M. J. Feldman and S. Rudner, "Mixing with SIS arrays," in *Reviews of Infrared & Millimeter Waves*, vol. 1. New York: Plenum, 1983, p. 47–75.
[12] L. R. D'Addario, "An SIS mixer for 90–120 GHz with gain and wide bandwidth," *Int. J. Infrared Millimeter Waves*, vol. 5, no. 11, pp. 1419–1442, Nov. 1984.
[13] A. V. Räisänen, W. R. McGrath, P. L. Richards, and F. L. Lloyd, "Broad-band RF match to a millimeter-wave SIS quasi-particle mixer," *IEEE Trans. Microwave Theory Tech.*, vol. MTT-33, pp. 1495–1500, Dec. 1985.
[14] S.-K. Pan, A. R. Kerr, J. W. Lamb, and M. J. Feldman, "SIS mixers at 115 GHz using Nb/Al-Al_2O_3/Nb junctions," Electronics Division Internal Report, No. 268, National Radio Astronomy Observatory, Charlottesville, VA 22903, Mar. 1987.
[15] A. R. Kerr. S.-K. Pan, and M. J. Feldman, "Integrated tuning elements for SIS mixers," *Int. J. Infrared Millimeter Waves*, vol. 9, no. 2, pp. 203–212, Feb. 1988. Presented at the Int. Superconductivity Electron. Conf., Tokyo, Japan, Aug. 1987.
[16] D. P. Woody, private communication, 17 May 1983.
[17] Li Xizhi, P. L. Richards, and F. L. Lloyd, "SIS quasiparticle mixers with bow-tie antennas," *Int. J. Infrared Millimeter Waves*, vol. 9, no. 2, pp. 101–133, Feb. 1988.
[18] R. L. Kautz, "Miniaturization of normal-state and superconducting striplines," *J. Res. Nat. Bur. Stand.*, vol. 84, no. 3, pp. 247–259, May–June 1979.
[19] T. Van Duzer and C. W. Turner, *Principles of Superconductive Devices and Circuits*. New York: Elsevier North Holland, 1981.
[20] R. E. Matick, *Transmission Lines for Digital and Communication Networks*. New York: McGraw-Hill, 1969.
[21] R. L. Sandstrom, A. W. Kleinsasser, W. J. Gallagher, and S. J. Raider, "Josephson integrated circuit process for scientific applications," *IEEE Trans. Magn.*, vol. MAG-23, no. 2, pp. 1484–1488, Mar. 1987.
[22] S.-K. Pan, M. J. Feldman, A. R. Kerr, and P. Timbie "Low-noise 115-GHz receiver using superconducting tunnel junctions," *Appl. Phys. Lett.*, vol. 43, no. 8, pp. 786–788, 15 Oct. 1983.
[23] S.-K. Pan and A. R. Kerr, "A superconducting tunnel junction receiver for millimeter-wave astronomy," NASA Technical Memorandum 87792, July 1986.
[24] P. H. Siegel, D. W. Peterson, and A. R. Kerr, "Design and analysis of the channel waveguide transformer," *IEEE Trans. Microwave Theory Tech.*, vol. MTT-31, pp. 473–484, June 1983.
[25] Alpha Metals, Jersey City, NJ 07305.
[26] Superior Flux & Mfg. Co., Cleveland, OH 44143.
[27] R. L. Eisenhart and P. J. Khan, "Theoretical and experimental analysis of a waveguide mounting structure," *IEEE Trans. Microwave Theory Tech.*, vol. MTT-19, pp. 706–719, Aug. 1971. A useful discussion is also given in: R. L. Eisenhart, "Understanding the waveguide diode mount," in *1972 IEEE Int. Microwave Symp. Dig.*, May 1972, pp. 154–156.
[28] R. L. Eisenhart, "Discussion of a 2-gap waveguide mount," *IEEE Trans. Microwave Theory Tech.*, vol. MTT-24, pp. 987–990, Dec. 1976.
[29] W. R. McGrath, A. V. Räisänen, P. L. Richards, R. E. Harris, and F. L. Lloyd, "Accurate noise measurements of superconducting quasiparticle array mixers," *IEEE Trans. Magn.*, vol. MAG-21, pp. 212–215, Mar. 1985.
[30] Infrared Laboratories, Inc., Tucson AZ, 85719, model HD-3(8), modified.
[31] V. Summers, "Chemistry laboratory procedures, 1988," NRAO Chemical Laboratory Report #7, National Radio Astronomy Observatory, Charlottesville, VA 22903, 18 Jan. 1988.
[32] W. L. Gore & Associates, Inc., Newark, DE 19711. Tetra-Etch.
[33] Emerson & Cuming, Inc., Canton, MA 02021. Eccobond 45 (clear), 100 parts by weight, Catalyst 15 (clear), 300 parts, cured 8 hours at room temperature.
[34] S.-K. Pan, M. J. Feldman, A. R. Kerr, E. S. Palmer, J. A. Grange and P. Timbie, "Superconducting tunnel junction receiver for 2.6 mm," in *Dig. 8th Int. Conf. Infrared and Millimeter Waves*, Dec. 1983, pp. M6.2/1–2.
[35] Dynatech-U/Z Inc., Calabasas, CA 91302, model M4-413C901.
[36] Passive Microwave Technology (Pamtech), Canoga Park, CA 91304, models 1102 (isolator) & 1141 (circulator).
[37] M/A-Com Omni Spectra Inc., Merrimack, NH 03054, model 2023-6123-20.
[38] Hewlett Packard, Inc., Palo Alto, CA 94303, models 8493A-20 dB & 8493A-30 dB.
[39] Servometer Corp., Cedar Grove, NJ 07009, model #1571-2, modified by removing the flange.
[40] EMC Technology, Inc., Cherry Hill, NJ 08034, model 4120J. Specify nichrome resistor element, as current version may have TaN element whose resistance may vary appreciably near 4 K. (Ta_xN_y can be superconducting with a critical temperature in the range 3.6–4.4 K.)
[41] M. W. Pospieszalski, S. Weinreb, R. D. Norrod, and R. Harris, "FET's and HEMT's at cryogenic temperatures: Their properties and use in low-noise amplifiers," *IEEE Trans. Microwave Theory Tech.*, vol. 36, pp. 552–560, Mar. 1988.
[42] H. B. Callen and T. A. Welton, "Irreversability and generalized noise," *Phys. Rev.*, vol. 83, no. 1, pp. 34–40, July 1951.
[43] M. J. Feldman, "Quantum noise in the quantum theory of mixing," *IEEE Trans. Magn.*, vol. MAG-23, pp. 1054–1057, Mar. 1987.
[44] R. Trambarulo and M. S. Berger, "Conversion loss and noise temperature of mixers from noise measurements," in *IEEE MTT-S Int. Microwave Symp. Dig.*, 1983, pp. 364–365.
[45] M. J. Feldman, S.-K. Pan, and A. R. Kerr, "Saturation of the SIS mixer," to be published.
[46] M. J. Feldman and L. R. D'Addario, "Saturation of the SIS direct detector and the SIS mixer," *IEEE Trans. Magn.*, vol. MAG-23, pp. 1254–1258, Mar. 1987.
[47] L. R. D'Addario, "Saturation of the SIS mixer by out-of-band signals," *IEEE Trans. Microwave Theory Tech.*, vol. MTT-26, pp. 1103–1105, June 1988.
[48] M. J. Feldman, S.-K. Pan, and A. R. Kerr, "Saturation of the SIS mixer," in *Proc. Int. Superconductivity Electron. Conf.* (Tokyo), Aug. 1987, pp. 290–292.

✠

Shing-Kuo Pan (S'81–M'85) was born in Taiwan, Republic of China, in 1953. He received the B.A. degree in physics from Fu-Jen University, Taiwan, in 1976 and the Ph.D. degree from Columbia University, New York, NY, in 1984.

Since 1984 he has been with the National Radio Astronomy Observatory, Charlottesville, VA, where he has been involved in research on SIS detectors and the development of SIS heterodyne receivers for radio astronomy. His other interests include computer-aided design, superconducting device fabrication techniques, and noise mechanisms in superconducting devices.

✠

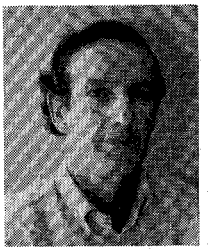

Anthony R. Kerr (S'64–A'66–SM'78–F'84) was born in England in 1941. He received the B.E., M.Eng.Sc., and Ph.D. degrees from the University of Melbourne, Australia, in 1964, 1967, and 1969, respectively.

In 1969, he joined the Commonwealth Scientific and Industrial Research Organization, Sydney, Australia, to develop cryogenic parametric amplifiers for radio astronomy at *X*-band. From 1971 to 1974, he worked at the National Radio Astronomy Observatory, Charlottesville, VA, developing the first cryogenically cooled Schottky-diode mixer receiver for millimeter-wavelength radio astronomy. Between 1974 and 1984, at the

NASA/Goddard Institute for Space Studies, New York, he worked on the theory and design of Schottky, Josephson, and SIS mixers for millimeter-wave receivers. In 1984, he returned to the National Radio Astronomy Observatory, where he is responsible for the development of new low-noise millimeter-wave receiver technology.

Dr. Kerr is a member of URSI Commission J and the Astronomical Society of Australia. He was a corecipient of the 1978 IEEE Microwave Prize and received the 1983 NASA Exceptional Engineering Achievement Medal.

Marc J. Feldman (M'88) was born in Philadelphia, PA, in 1945. He received the B.A. and M.S. degrees in physics from the University of Pennsylvania, both in 1967, and the Ph.D. degree in physics from the University of California at Berkeley in 1975.

He has specialized in device-oriented theoretical research related to high-frequency applications of superconductivity since 1971, and was co-originator of the inverse ac Josephson effect voltage standard and the unbiased Josephson parametric amplifier. Other topics of research have included optical parametric interactions, electron acceleration by lasers, interstellar extinction, and astronomical observations of the CN radical.

From 1979 to 1985 he worked with groups researching SIS mixers at Chalmers University in Gothenburg, Sweden, and at the NASA/Goddard Institute for Space Studies, contributing to the understanding and successful development of SIS receivers for various radio astronomy observatories. Since 1985 he has been Research Associate Professor of Electrical Engineering at the University of Virginia, where he leads an effort to develop SIS junctions for receiver applications.

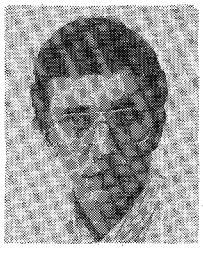

Alan W. Kleinsasser received the B.S. degree from the California Institute of Technology in 1974, and the M.S. and Ph.D. degrees from Cornell University in 1976 and 1980, all in applied physics. His doctoral work focused on superconductive tunnel junctions and included the development of several techniques for fabricating submicron high-current-density Josephson junctions.

He joined the Exploratory Cryogenics program at the IBM T. J. Watson Research Center in 1980 as Research Staff Member, where he worked on various aspects of Josephson integrated circuit technology development until the program closed in 1983. Since then he has continued to pursue research in cryogenics, primarily on exploratory three-terminal devices such as superconductor–semiconductor hybrids and semiconductor heterostructures, with ongoing participation in Josephson device and circuit fabrication for scientific applications and, more recently, in studies of high-temperature superconductors.

Dr. Kleinsasser is a member of the American Physical Society, the American Vacuum Society, and the Materials Research Society.

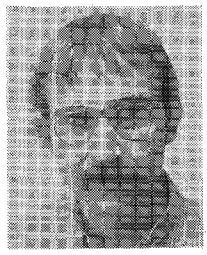

James W. Stasiak was born in Chicago, IL, in 1954. He received the B.A. degree in physics from Lewis University, Lockport, IL, in 1977 and the M.S. degree in physics from Southern Illinois University, Carbondale, IL, in 1979. He is currently working towards the Ph.D. degree in electrical engineering at Yale University, New Haven, CT.

He joined the IBM T. J. Watson Research Center, Yorktown Heights, N.Y. in 1979, where he has been involved with circuit design and measurements related to Josephson integrated circuit technology. He is currently a research staff engineer in the Insulator Physics group, and his research interests include the characterization of mobility-limiting scattering mechanisms in thin gate dielectric MOSFET's and quantum mechanical effects in inversion layer transport.

Mr. Stasiak is a member of the American Physical Society.

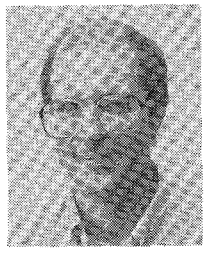

Robert L. Sandstrom (A'84) received the B.S. degree in industrial technology from the University of Wisconsin-STOUT, Menomonie, in 1975, with specialities in research physics and electronics.

He then joined the AMOCO Research Center, Naperville, IL, as a member of the Advanced Energy Group responsible for metal hydride R&D. In 1980 he joined the Materials Research Corporation, Pearl River, NY, as a Technical Associate Engineer working on the R&D of a magnetron plasma tool for characterization and single wafer etching, for which he received a special company award. Since 1984, he has been at the IBM T. J. Watson Research Center, Yorktown Heights, NY, in the Exploratory Cryogenics group. He is a Senior Associate Engineer, responsible for Josephson integrated circuit fabrication for scientific applications. More recently he has been involved in the field of high-temperature superconductivity, developing a reliable low-pressure magnetron sputtering process for fabricating thin films and dc SQUID devices.

Mr. Sandstrom is a member of the AVS, APS, and Tesla societies.

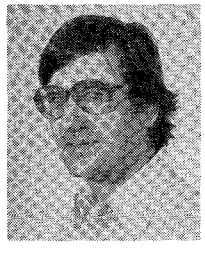

William J. Gallagher (M'84) received the B.S. degree in physics from Creighton University in 1974 and the Ph.D. degree, also in physics, from MIT in 1978.

Since 1978, he has been employed at the IBM T. J. Watson Research Center, Yorktown Heights, NY. He worked for five years on engineering and scientific aspects of Josephson computer technology within a development program. After the termination of that program, he was engaged in new superconducting device research and, more recently, worked on the problems of understanding the basic properties and applications potential of the new high-temperature superconductors. He is currently the manager of an Exploratory Cryogenics group at IBM.

Dr. Gallagher is a member of the American Physical Society (APS). He has worked for the APS Panel on Public Affairs and served a two-year elected term on the Executive Committee of the APS Forum on Physics and Society. In 1986 he was elected to a six-year term on the Board of Directors of the Applied Superconductivity Corporation.